



Published in final edited form as:

*J Opt Soc Am A Opt Image Sci Vis.* 2020 April 01; 37(4): A26–A34. doi:10.1364/JOSAA.381919.

## Tritan color vision deficiency may be associated with an *OPN1SW* splicing defect and haploinsufficiency

Maureen Neitz<sup>1,\*</sup>, Elise D. Krekling<sup>2</sup>, Lene A. Hagen<sup>2</sup>, Hilde R. Pedersen<sup>2</sup>, Jessica Rowlan<sup>1</sup>, Rachel Barborek<sup>1</sup>, Jay Neitz<sup>1</sup>, Adam Crain<sup>1</sup>, Rigmor C. Baraas<sup>2</sup>

<sup>1</sup>University of Washington, Department of Ophthalmology, 750 Republican Street, Seattle, WA, USA 98109

<sup>2</sup>National Centre for Optics, Vision and Eye Care, Faculty of Health and Social Sciences, University of South-Eastern Norway, Kongsberg, Norway.

### 1. INTRODUCTION

Inherited tritan color vision deficiencies exhibit an autosomal dominant inheritance pattern and are caused by mutations in the short-wavelength sensitive (S) cone opsin gene (*OPN1SW*) [1–5]. There are six known mutations associated with inherited tritan color vision defects. These are the substitution of proline for leucine at amino acid position 56 (L56P), arginine for glycine at position 79 (G79R), proline for serine at position 214 (S214P), serine for proline at position 264 (P264S), isoleucine for threonine at position 190 (T190I), and glutamine for arginine at position 283 (R283Q). Adaptive optics imaging of related individuals affected by the R283Q mutation suggested a progressive S cone degeneration that is correlated with progressively deteriorating blue-yellow color vision, thus providing the first evidence that inherited tritan color vision deficiencies are not congenital [5] and can be progressive with regard to color vision loss.

Here, we identified an individual whose color vision test results are consistent with the presence of an inherited tritan color vision deficiency. She is heterozygous for a nucleotide deletion in intron 3 of the *OPN1SW* gene that disrupts the consensus 5' splice site and is thus expected to cause an RNA splicing defect. This mutation was first reported by Weitz and colleagues [1, 2] in a family (family C in [1]) that was previously shown to be segregating inherited tritanopia [6]. The genetic analysis, performed about a decade after the initial diagnosis, revealed that the family was segregating the intron 3 nucleotide deletion and the P264S mutation which was shown to cause tritanopia on its own in an unrelated family [1, 2]. Members of family C who had the P264S and a normal allele had tritanopia, as did members of the family who had the P264S and the nucleotide deletion allele. Color vision test results were not reported for members of the family who had the nucleotide deletion and a normal allele [6], but Weitz and colleagues concluded that the nucleotide deletion is not associated with tritanopia [6]. However, they did not entertain the possibility

\*corresponding author: mneitz@uw.edu.

6.2 Disclosures

The authors declare no conflicts of interest

that the nucleotide deletion might cause a milder color vision deficit, nor did they determine whether the nucleotide deletion disrupts splicing. Results reported here demonstrate that the *OPN1SW* intron 3 nucleotide deletion causes a splicing defect such that heterozygous individuals are expected to have S cones with a reduced amount of opsin protein compared to normal, and that the mutant is associated with tritan color vision deficiency that is mild compared to the P264S mutation.

## 2. METHODS

### 2.1 Subjects and Color Vision Testing

Human subjects were recruited through the National Centre for Optics, Vision and Eye Care at the University of South-Eastern Norway in Kongsberg. Informed consent was obtained from all subjects. Experiments involving human subjects conformed to the principles expressed in the Declaration of Helsinki (Code of Ethics of the World Medical Association) and was approved by the Regional Committee for Medical and Health Research Ethics (South-Eastern Norway Regional Health Authority). Color vision testing was performed in Norway; genetic testing was performed in the U.S.A. at the Medical College of Wisconsin (MCW) or the University of Washington (UW). De-identified blood or saliva samples were shipped to these locations for genetic analysis of the cone opsin genes. Work performed at MCW and UW was approved by Institutional Review Boards at each institution.

Color vision testing was initially performed on 51 subjects. One subject, ID #4028, made tritan errors, and thus her sister and mother were recruited to the study. All subjects participated in testing using the Richmond Products Hardy-Rand-Rittler (HRR) 4th edition pseudoisochromatic plate test and Farnsworth-Munsell (FM) 100 Hue, and 49 were tested using the Cambridge Colour Test (CCT) using standard procedures. All subjects had normal ophthalmic examinations and normal or corrected-to-normal visual acuity (logMAR 0.0 or better) (for details see [7]).

### 2.2 Genetic Analyses and Bioinformatics Analyses

Whole blood drawn in buffered citrate or saliva collected using the Oragene kit (DNA Genotek, Ottawa, Canada) was obtained from each subject. DNA was extracted from blood using the 5PRIME blood DNA extraction kit (Thermo Fisher, Waltham, MA), and from saliva using the PrepIt L2P saliva DNA extraction kit (DNA Genotek). DNA from each subject was used in the polymerase chain reaction (PCR) to amplify each exon of the *OPN1SW* gene and about 50 base pairs of the flanking introns. PCR primers are shown in Table 1. As indicated in the table, we discovered a mismatch with the *OPN1SW* reference sequence for one of the primers, however, such mismatches are commonly intentionally incorporated for experimental reasons, and have no significant impact on the primer's function unless the mismatch is at the 3' end, which this is not [8]. Amplification was performed using the Platinum Taq PCR kit (Thermo Fisher, Waltham, MA). Reactions were first incubated at 95°C for 5 minutes, followed by 37 cycles of 94°C for 45 seconds, 58°C for 45 seconds, and 72°C for 45 seconds, followed by 1 cycle at 72°C for 7 minutes. PCR amplified DNA was purified and sequenced directly on both strands using the ABI Prism BigDye Terminator sequencing kit, version 3.0. Sequencing primers were the same as those

used for amplification and sequencing reactions were analyzed on an ABI 3500 Genetic Analyzer.

Each nucleotide variation observed in the subject pool was evaluated for its potential effect on splicing using the online bioinformatics tools, Human Splicing Finder 3.1 [9] and Mutation Taster [10]. Human Splicing Finder identifies motifs that can serve as exonic splicing enhancers (ESEs) or exonic splicing silencers (ESSs), and splicing donor and acceptor sites. Mutation taster evaluates the likelihood that a mutation is disease causing both with regard to potential effects on splicing and on protein structure and function.

## 2.3 Splicing Assays

**2.3.1 Transient transfections using plasmids carrying the gene for *OPN1SW* or rhodopsin**—In vitro splicing assays are widely used in instances where patient somatic cells are not available, or the gene of interest is not expressed in accessible somatic cells, as is the case here [11, 12]. The most common approach is to introduce plasmids carrying the gene of interest into human cells in culture via transient transfection [13]. We created plasmids carrying the *OPN1SW* gene variants found in subjects in this study, and a plasmid carrying the gene for rhodopsin as a control. We chose rhodopsin as the control because the wild-type rhodopsin gene has previously been shown to splice correctly in splicing assays [14] and it is similar in size and structure to the *OPN1SW* gene [15, 16].

Plasmids were created by first using PCR to amplify the corresponding gene from genomic DNA from subjects. *OPN1SW* was amplified with the forward primer ATCATGCGGCCGCATGAGAAAAATGTCGGAGG, and the reverse primer GCGACGTCGACATTTAATTCTAGCTGTTGC. The rhodopsin gene was amplified with the forward primer GATCATGCGGCCGCCTTCGCAGCATTCTTGGGT and the reverse primer GCGACGTCGACTTAATACCAACATAGGAGCTG. The underlined sequences in the forward primers are *Not*I restriction enzyme cleavage sites, and the underlined sequences in the reverse primers are *Sal*I restriction enzyme cleavage sites. These restriction sites were used for cloning the amplicons. The *OPN1SW* gene was amplified using a first denaturation step at 94°C for 2 minutes, followed by 25 cycles of 94°C for 30 seconds, 60°C for 30 seconds, 68°C for 2 minutes and a final extension step of 68°C for 4 minutes. The rhodopsin gene was amplified with a first denaturation step at 94°C for 2 minutes, followed by 25 cycles of 94°C for 30 seconds, 60°C for 30 seconds, 68°C for 1 minute and a final extension step of 68°C for 3 minutes. PCR was performed using the Platinum Taq HiFi enzyme and PCR reagents (Invitrogen, Carlsbad, CA), and the products were purified with the Quickstep PCR purification spin columns (EdgeBio, Gaithersburg, MD). The purified PCR products were digested with restriction enzymes *Not*I and *Sal*I, as was the cloning vector pFLAG-CMV $\alpha$  (Sigma-Aldrich, St. Louis, MO). The PCR amplified genes were ligated into the cloning vector, and the mixtures were used to transform *E. coli* cells. Plasmids were purified from the *E. coli* and sequence verified.

Plasmids carrying an *OPN1SW* gene or the rhodopsin gene were transfected into HEK293 cells (American Type Culture Collection, Manassas, VA) using FuGene HD (Promega, Madison, WI). Wells were cultured in Dulbecco's modified Eagle's Medium (Gibco Laboratories, Gaithersburg, MD) containing 10% HyClone Cosmic Calf serum (Thermo

Fisher, Waltham, MA). Duplicate wells of HEK293 cells were transfected with each of the opsin gene clones, and total RNA was isolated from cells 48 hours later using the Nucleospin RNA kit (Clontech, Mountain View, CA). RNA was treated with DNase I to remove contaminating DNA, ethanol precipitated, and converted to copy DNA (cDNA) by reverse transcribing (RT) using PrimeScript first strand synthesis kit (Clontech, Mountain View, CA). Two microliters of the RT reaction were used for PCR with the same forward and reverse primers used to create the *OPN1SW* plasmids (see above) and with forward primer 5'GCTCAGGCCTTCGCAGC and reverse primer 5'GTGGCTGACTCCTGCTGCTGGG for rhodopsin. The RT-PCR products were analyzed by agarose gel electrophoresis. The DNA bands observed were extracted from the gel and directly sequenced to identify the splicing isoforms. Sequencing was performed using the BigDye Terminator 3.1 kit, following the manufacturer's recommendations (Thermo Fisher, Waltham, MA). The sequencing reactions were analyzed using the ABI 3500 genetic analyzer (Applied Biosystems, Foster City, CA).

**2.3.2 Stable cell lines**—Normally, genes are transcribed from the context of a chromosome; however, in transiently transfected cells, plasmids are maintained episomally and it is possible that this could inhibit accessibility of the splicing machinery to the plasmid-borne genes. As a control, to validate the splicing assay results obtained using transiently transfected cells for the *OPN1SW* gene, we made isogenic stable cell lines expressing the *OPN1SW* full-length gene integrated into chromosomal DNA using the Flp-In HEK293 host cell line and the Flp-In kit (Invitrogen, Carlsbad, CA). The Flp-In HEK293 host cell line has a single FRT site integrated into genomic DNA. The PCR amplified *OPN1SW* gene from the control subject was first cloned into the Flp-In expression plasmid, pcDNA5/FRT and sequence verified. The plasmid was then co-transfected into HEK293 Flp-In host cells with the Flp recombinase expression plasmid, pOG44. A stable cell line (CMV\_*OPN1SW*\_Flp-In HEK293) with the *OPN1SW* gene under control of the CMV promoter integrated at the host cell's FRT site was isolated and verified according to the manufacturer's protocol. The integrated *OPN1SW* gene is under control of the ubiquitous CMV promoter, whereas the endogenous *OPN1SW* gene is under control of a cone-specific promoter. Thus, only the integrated *OPN1SW* gene is expressed in the CMV\_*OPN1SW*\_Flp-In HEK293 cells.

Total RNA was isolated from the CMV\_*OPN1SW*\_Flp-In HEK293 cells, reverse transcribed as described above for transient transfections. The RT-PCR products were examined by gel electrophoresis and sequencing. The RT-PCR products were also ligated into plasmid pFLAG-CMV $\alpha$ , and the ligation reaction was used to transform *E. coli* DH5 $\alpha$  cells (Thermo Fisher, Waltham MA). Colony PCR was performed using Dream Taq (Thermo Fisher, Waltham, MA), and incubating for a first denaturation step at 95°C for 2 minutes, followed by 25 cycles of 95°C for 30 seconds, 60°C for 30 seconds, and 72°C for 1.5 minutes, and a final extension step at 72°C for 3 minutes. Between 40 and 100 colonies were subjected to colony PCR and sequencing in order to characterize the different splicing isoforms obtained, and to quantify their relative amounts.

**2.3.3 Order of intron removal**—Using the CMV\_*OPN1SW*\_Flp-In HEK293 cell, the order of intron removal from the *OPN1SW* gene was investigated. The primers used in the analysis, including their locations and melting temperatures ( $T_m$ ) are given in Table 2. DNA-free RNA was isolated from the CMV\_*OPN1SW*\_Flp-In HEK293 cell line by first isolating total RNA, then treating it with DNase I. The DNase I treated RNA was used in RT-PCR with random hexamers to prime the reverse transcriptase reaction. RT-PCR was also done in the absence of reverse transcriptase to verify that the products observed were from RNA, not contaminating DNA. The same amount of RNA was used in each RT-PCR reaction, and 10  $\mu$ l of the RT-PCR product was subjected to agarose gel electrophoresis.

## 3.0 RESULTS

### 3.1 Color vision testing results

None of the subjects made errors on the HRR 4th edition test. The Color vision test results for the putative tritan, subject 4028 and her mother and sister are shown in Figure 1 and Table 3. The scoring system for the FM100 Hue test is that described by Kinnear and Sahraie [17]. The blue-yellow (BY) total partial error score (TPES) is based on the scoring mechanism applied to caps 1–12, 34–54 and 76–85 [17]. Subject 4028 was initially tested at age 24 years and again at 32 years. She made tritan errors on the FM100 Hue and CCT tests. Her age-adjusted total error score (TES) on the FM100 Hue was outside the 95% confidence limits for the distribution of the other subjects (Figure 1). This was also true for her performance on the FM100 Hue B/Y caps and the CCT tritan vector.

The sister and mother of subject 4028 agreed to participate in color vision testing. The sister (subject 4069) was tested at age 27 years, and her results on the CCT were similar to those for subject 4028 (Table 3). However, her error scores on the FM100 Hue test and on the FM100 B/Y caps (TPES in Table 3) were above the mean for the 50 normal subjects but within the 95% confidence limits (Figure 2). The mother of 4028 and 4069 (subject 5204) was tested at age 71 years on the FM100 Hue. She had had cataract surgery at age 66 years and was recently diagnosed with early age-related macular degeneration. Her age-adjusted total error score was above the mean for the 50 normal subjects, but within the 95% confidence interval, however on the FM100 Hue B/Y caps, her error score was below the mean for the other subjects (Figure 2).

### 3.2 Genetic and bioinformatics analysis

We sequenced the exons and ~50 base pairs (bp) of the flanking introns of the *OPN1SW* genes for the 53 subjects who participated in color vision testing. The 53 subjects are the initial 51 subjects plus the mother and sister of the original subject who made tritan errors. A total of four nucleotide variations were observed, and these are mapped onto an illustration of the *OPN1SW* gene in Figure 3, and summarized in Table 4. The variations at c.31, c.222, and c.366 are the most common exonic polymorphisms that have been identified in the *OPN1SW* gene in large population studies [18]. All three are nucleotide polymorphisms in exons that do not alter the amino acid sequence and thus have no functional consequences for protein structure or function. One subject was heterozygous at exon 1 nucleotide position c.31C>T, where T is the minor allele with a population frequency of 0.67%. Another subject

was heterozygous at exon 1 nucleotide position c.222C>A, where A is the minor allele with a population frequency of 0.91%. Nineteen subjects were heterozygous at exon 2 position c.366A>C, where C is the minor allele with a population frequency of 30%. Twenty-four were homozygous for c.366A and nine were homozygous for c.366C.

The subject who made significant tritan errors (ID# 4028) and her mother and sister (ID#s 4069 and 5204, respectively) were all heterozygous for the deletion of a G residue in intron 3, five base pairs downstream of the 3' end of exon 3 (see Figure 3). The deletion, abbreviated exon 3 +5G deletion, affects a nucleotide that is part of the 5' splicing signal for intron 3 and thus has the potential to disrupt pre-messenger RNA splicing and the minor allele frequency is estimated to be 0.132% in large population studies [18]. The fact that 1 of 1 proband had an *OPN1SW* mutation compared to 0 of 50 control subjects (Fisher's exact test  $p = 0.0385$ ) along with the familial segregation of a mild tritan color vision defect and the *OPN1SW* gene mutation in the two additional relatives of the proband, provides support for the conclusion that the *OPN1SW* gene mutation is the cause of the mild tritan deficiency in these individuals.

Human Splicing Finder predicts [9] that the deletion most probably affects splicing. The only absolutely conserved portion of the 5' splice site consensus sequence is the first two nucleotides of the intron. The consensus sequence for the 5' splice site in humans is CAG/guragu (the exon sequence is given in upper case, and the adjacent intron is given in lower case, and r designates an a or g nucleotide). This sequence is complimentary to U1 snRNA, which is part of the basal splicing machinery present in every cell. Deletion of the G that is the fifth residue of the intron results in a T (U in RNA) at the fifth position. G is predominantly found at this position in human introns; however, about 25% of "normal" exons do not have a G at this position of the 5' splice site [19]. Furthermore, simulation of all possible nucleotide substitutions at the 5' splice site for all human exons using a splicing algorithm that showed 97.1% sensitivity and 94.7% specificity predicted that a nucleotide change at the +5 position will cause aberrant splicing 96.5% of the time [20]. Thus, based on the *in silico* analysis, there is a high likelihood that the exon 3+5G deletion in *OPN1SW* will cause aberrant splicing.

Human splicing finder also predicted that the other three observed nucleotide polymorphisms alter sequence motifs that may be important for splicing. The c.31C>T change creates an exonic splicing silencer (ESS), the c.222C>A and c.366A>C substitutions each disrupt exonic splice enhancers (ESEs), and the c.222C>A change also creates a cryptic, albeit weak, splice donor site. The c.31C>T, c.222C>A, and c.366A>C changes were also analyzed by mutation taster [10], which predicted that the c.222C>A and c.31C>T changes may be disease causing due to potential influences on splicing, but that the c.366A>C change likely represents a benign polymorphism based on its prevalence in the population and the absence of known disease associations.

### 3.4 Splicing Assay

Due to the degeneracy of splicing signals, the effects of nucleotide variations on splicing cannot be accurately predicted from *in silico* analysis of sequence data alone, thus *in vitro* splicing assays were performed to assess the potential role of exon 3 +5G deletion on

splicing. Figure 4 shows the results obtained for *OPN1SW* variants transiently transfected into HEK293 cells. The exon 3 +5G deletion gave a very clear result in that a single splicing isoform was observed by gel electrophoresis (Figure 4A). Direct sequencing of this product revealed that it represents a single isoform that lacks exons 2 and 3, and contains exon 1, 4 and 5 spliced together (Figure 4B). This creates a frameshift in the protein code starting at codon 119, and introduces a premature translation termination codon at position 133 (abbreviated fs119\_X133). This result predicts that individuals heterozygous for the exon 3 +5G deletion mutant will have S cones that contain half the normal amount of opsin protein because the aberrantly spliced transcript does not encode a functional opsin.

In the 50 normal subjects, four different *OPN1SW* alleles were identified: one that is most common in the population, and three minor alleles that contained a nucleotide substitution at one of three positions (c.31, c.222, c.366). The major allele had c.31C, c.222C and c.366A. Each of the three minor alleles differed from the major allele at one position. One had c.31T, one had c.222A, and one had c.366C. All yielded multiple splicing isoforms and the same banding pattern as the normal *OPN1SW* gene shown in Figure 4A lanes 3 through 5. Splicing products obtained from a clone of the rhodopsin gene was also analyzed as a control. The rhodopsin gene gave rise to a single product, that upon sequencing proved to be correctly spliced.

To assess the possibility that the multiple splicing isoforms observed from the *OPN1SW* gene are due to the *OPN1SW* gene being in the context of a plasmid instead of a chromosome, we created a cell line with the *OPN1SW* gene integrated into a chromosome, and characterized the splicing isoforms obtained from the integrated gene. The banding pattern observed for *OPN1SW* splicing isoforms obtained from the CMV\_*OPN1SW*\_FLP-In HEK293 cells was the same as that observed for transiently transfected cells.

For RT-PCR products representing the splicing isoforms from both the transiently transfected cells and CMV\_*OPN1SW*\_Flp-In HEK293 cells, the different bands observed were gel purified, and directly sequenced. Only the lowest molecular weight band clearly contained a single PCR product, which was the isoform in which both exons 2 and 3 were missing. The other two bands contained mixtures of multiple splicing isoforms. To characterize the splicing isoforms produced, we cloned the *OPN1SW* RT-PCR products from the CMV *OPN1SW*\_Flp-In HEK293 cell line, and sequenced 65 different clones. Sixty-two percent (n = 40) of the clones contained the full length, correctly spliced form, 23% (n = 15) were the exon 2 skipped form, 7–8% (n = 5) lacked exon 2 and 3, and 7–8% (n = 5) lacked exons 2, 3 and 4.

### 3.5 Order of Intron Removal

We predict that the exon 3 +5G deletion disrupts the 5' splice site in exon 3, and will simply cause exon 3 skipping. However, previous studies have shown that other splicing isoforms, such as multi-exon skipping, might be obtained as a consequence of the order in which the introns are normally removed [21]. In order to evaluate whether the order in which the introns are spliced out of the *OPN1SW* pre-mRNA contributes to the specific splicing isoforms observed, we determined the relative order in which introns are removed from the *OPN1SW* gene during splicing in the CMC\_*OPN1SW*\_Flp-In HEK293 cells. In this

experiment, pairs of primers are used such that one primer binds to an intron and the other binds to an exon. The RT-PCR products observed are all splicing intermediates. The potential splicing intermediates for each primer pair used, are illustrated in Figure 5. Those that were not observed in the experiments for which results are shown in Figure 6, are not actual splicing intermediates, whereas all the products that were observed are true splicing intermediates.

In Figure 6A, using a forward primer to exon 1 and a reverse primer to intron 2, only the 736 bp splicing intermediate is observed, but using a forward primer in intron 1 and a reverse primer in exon 2, both the 822 bp and 500 bp splicing intermediates are observed. Together these results indicate that intron 1 is not removed until after intron 2 is spliced out. Using a primer that binds in exon 1 and a reverse primer that binds in intron 3 (Figure 6B), yields three of the five potential splicing intermediates shown in Figure 5. The 1338 bp splicing intermediate has introns 1, 2 and 3, but the absence of the 1016 and 1056 bp bands demonstrate that there are not intermediates with introns 1 and 3 or with introns 2 and 3. There is an intermediate in which both introns 1 and 2 have been removed, and another in which intron 1, exon 2 and intron 3 have all been removed as one large intron. These results confirm that intron 1 is not spliced out before intron 2.

Using primers to exon 1 and intron 3, the 1016 bp intermediate in which intron 2 has been removed, but intron 1 remains is not observed (Figure 6B), indicating that it either does not exist or is present in such low amount that we cannot detect it. However, using primers to intron 1 and exon 3, a 500 bp intermediate is detected (Figure 6A) in which intron 2 remains and intron 1 is removed. This suggests that the 1016 bp intermediate does exist, but in such low quantity that we cannot detect it, even with a very sensitive PCR assay. Together, these observations suggest that introns 1 and 2 may be removed in rapid succession with intron 2 removed first, and intron 1 second.

Using a forward primer in exon 2 and a reverse primer in intron 3 (Figure 6C) yields both of the potential splicing intermediates illustrated in Figure 5, as does using a forward primer in intron 2 and a reverse primer in exon 4 (Figure 5 and Figure 6). These findings do not reveal a preference for the relative order in which introns 2 and 3 are removed. The results in Figure 6E shows that intron 4 is removed before intron 3 because only the 389 bp splicing intermediate is observed. This is confirmed by the results in Figure 6F using a forward primer in intron 2 and a reverse primer in exon 5 since the 1539 bp potential splicing intermediate shown in Figure 5 is not observed.

The observation of the 500 bp intermediate seen with the primers to intron 1F and exon 2R is consistent with the lack of the 1016 and 1056 intermediates using the exon 1F and intron 3 R primers. Presumably the 500 bp species is part of an intermediate in which the only intron left to be removed is intron 1. In the aggregate, the results in Figure 6 indicate two possible orders in which the introns are removed: 4, 3, 2, then 1 or 4, 2, 1 then 3. Perhaps the most interesting result is that the normal *OPN1SW* gene shows a predisposition to exon 2 skipping.



## 4.0 Discussion and Conclusions

The major findings reported here are that in an initial group of 51 subjects who were tested for color vision, one made tritan errors on both the FM100 Hue test and the Cambridge Colour Test. She was found to be heterozygous for a mutation in the *OPN1SW* gene that was shown in an *in vitro* assay to cause a pre-mRNA splicing defect such that the mutant allele cannot give rise to functional mRNA or opsin protein. While a variety of pathologies can produce a mild color vision loss similar to what was observed in the putative tritan subjects in this study [22], the most likely explanation is the *OPN1SW* gene mutation.

The control *OPN1SW* alleles used in the splicing assay represent those found in the 50 subjects who were categorized as having normal trichromatic color vision and correspond to the three most common alleles observed in large population studies. All of them yielded the same complement of splicing isoforms. Quantitative analysis of one of the control *OPN1SW* alleles revealed that the major isoform was the correctly spliced, full length mRNA. Due to the splicing defect in the exon 3 +5G deletion *OPN1SW* allele, affected subjects are expected to have S cones with half the normal amount of S opsin, and the mechanism of tritan color vision deficiency caused by this mutation must be haploinsufficiency.

The mutation in the exon 3 +5G deletion *OPN1SW* allele disrupts a consensus splice site that is recognized by the basal splicing machinery, common to all eukaryotic cells [19]; however, the observation that both exon 2 and 3 are skipped rather than just exon 3 was unexpected. We investigated the order in which the introns are removed from the normal *OPN1SW* gene to determine whether this contributes to exon 2 and 3 skipping in the exon 3 +5G deletion mutant. The results show a predisposition for the normal *OPN1SW* alleles to skip exon 2. In the exon 3 +5G deletion mutant, intron 3 cannot be removed on its own because of the disrupted 5' splice site, thus intron 1, exon 2, intron 2, exon 3 and intron 3 are removed as one large intron, giving rise to the exon 2,3 skipped splicing isoform observed.

To address the question of whether the splicing isoforms of the normal *OPN1SW* alleles observed in the *in vitro* assay are likely to represent the splicing isoforms that would be obtained from human S cones, we performed the *in vitro* splicing assay on the human rhodopsin gene which is similar to the *OPN1SW* gene in the number and sizes of the introns and exons [15, 16]. It spliced perfectly in HEK293 cells. This is consistent with a previous report [23]. We and others have previously shown that the only measurable splicing isoform obtained from HEK293 cells for some haplotypes of *OPN1LW* and *OPN1MW* genes is also the correctly spliced mRNA [24–26]. Thus, HEK293 cells appear to have the appropriate machinery in general to produce the correctly spliced mRNA from human photopigment genes. Inefficient splicing appears to be a feature of the *OPN1SW* gene. The idea that the normal, common alleles of the human *OPN1SW* gene are inefficiently spliced is supported by the bioinformatics analysis that identifies each of the polymorphic nucleotide positions as being associated with motifs that can facilitate or inhibit splicing, and because of their locations, these nucleotide polymorphisms would affect splicing of introns 1 and 2. The fact that the *OPN1SW* normal alleles are predisposed to skipping exon 2 also supports the role of these nucleotide positions in splicing.

How might haploinsufficiency cause tritan color vision deficiency? The S-cones have significant disadvantages compared to L and M cones. They only make up about 6% of all cones [27]. Compared to L and M cones, a much larger portion of light incident on the cornea to which the S-cones are sensitive is lost to absorption by the crystalline lens and the macular pigment. We calculated the relative amount of photons available to S cones compared to L and M cones in the human retina, using the CVRL macular pigment density spectra and lens density spectra [28] and the L, M and S cone fundamentals from Carroll et al. [29]. In young healthy adults, taking into account both the absorption of the lens and the macular pigment, for an equal energy white light, only about 9% of the photons reaching the L cones and 12% reaching the M cones are available to the S-cones. Furthermore, the results presented here suggest that S-opsin RNA splicing may be inefficient in normal S-cones such that they contain only about 60% of the photopigment of most normal L and M cones, thus, reducing photon catch. The combined effects of many fewer available photons because of preretinal absorption multiplied by the lower than normal optical density may make the S-cones vulnerable to anything that further reduces quantal catch. In support of this idea, is the observation by many groups independently that both with age-related yellowing of the lens, which reduces the amount of short wavelength light reaching the S-cones, and with reduced illumination, the largest change in error score on the FM100 Hue test [30–32] and on the Cambridge Colour Test is on the tritan axis [33, 34]. In the case of the exon 3 +5G deletion mutation, it appears that one of the two *OPN1SW* alleles produces no protein, which could reduce the optical density to half of normal. Consider the scenario that S-cones normally operate near their lower limits, then halving the amount of photopigment available to absorb light, this would be expected to result in loss of S-cone signals and manifest as a tritan defect.

Thus, haploinsufficiency might cause tritan color vision deficiency through a substantial reduction in the number of photons captured by S cones. Finally, variability in whether members of the same family with the exon 3 +5G deletion mutant manifest a tritan color vision defect may be based on factors such as diet that influence the density of the macular pigment, and on the presence of cataracts or removal of the lens as in the case of the mother of subjects 4028 and 4069.

## Funding

Work described here was supported in part by National Institutes of Health Grants P30EY001730, and R01EY028118, and by an unrestricted grant from Research to Prevent Blindness to the University of Washington Department of Ophthalmology. Maureen Neitz is the Ray H. Hill Professor in Ophthalmology, and Jay Neitz is the Bishop Professor in Ophthalmology. Work done at the University of South-Eastern Norway was supported by internal research funds.

## References

1. Weitz CJ, Went LN, and Nathans J, “Human tritanopia associated with a third amino acid substitution in the blue sensitive visual pigment,” *American Journal of Human Genetics* 51, 444–446 (1992). [PubMed: 1386496]
2. Weitz CJ, Miyake Y, Shinzato K, Montag E, Zrenner E, Went LN, and Nathans J, “Human tritanopia associated with two amino acid substitutions in the blue sensitive opsin,” *American Journal of Human Genetics* 50, 498–507 (1992). [PubMed: 1531728]

3. Gunther KL, Neitz J, and Neitz M, "A novel mutation in the short-wavelength sensitive cone pigment gene associated with a tritan color vision defect," *Visual Neuroscience* 23, 403–409 (2006). [PubMed: 16961973]
4. Baraas RC, Carroll J, Gunther KL, Chung M, Williams DR, Roster DH, and Neitz M, "Adaptive optics retinal imaging reveals S-cone dystrophy in tritan color vision deficiency," *Journal of the Optical Society of America A* 24, 1438–1447 (2007).
5. Baraas RC, Hagen LA, Dees EW, and Neitz M, "Substitution of isoleucine for threonine at position 190 of S-opsin causes S-cone-function abnormalities," *Vision Res* 73, 1–9 (2012). [PubMed: 23022137]
6. Higgins KE, Brooks DN, and Gottschalk G, "Tritan pedigree without optic-nerve atrophy," *Am J Optom Physiol Opt* 60, 964–969 (1983). [PubMed: 6606981]
7. Dees EW, Gilson SJ, Neitz M, and Baraas RC, "The influence of L-opsin gene polymorphisms and neural ageing on spatio-chromatic contrast sensitivity in 20–71 year olds," *Vision Res* 116, 13–24 (2015). [PubMed: 26368273]
8. Scharf SJ, "Cloning iwth PCR," in *PCR Protocols A Guide to Methods and Applications*, Innis MA, Gelfand DH, Sninsky JJ, and White TJ, eds. (Academic Press, 1990), pp. 84–91.
9. Desmet FO, Hamroun D, Lalonde M, Collod-Beroud G, Claustres M, and Beroud C, "Human Splicing Finder: an online bioinformatics tool to predict splicing signals," *Nucleic Acids Res* 37, e67 (2009). [PubMed: 19339519]
10. Schwarz JM, Cooper DN, Schuelke M, and Seelow D, "MutationTaster2: mutation prediction for the deep-sequencing age," *Nature methods* 11, 361–362 (2014). [PubMed: 24681721]
11. Sangermano R, Khan M, Cornelis SS, Richelle V, Albert S, Garanto A, Elmelik D, Qamar R, Lugtenberg D, van den Born LI, Collin RWJ, and Cremers FPM, "ABCA4 midigenes reveal the full splice spectrum of all reported noncanonical splice site variants in Stargardt disease," *Genome Res* 28, 100–110 (2018). [PubMed: 29162642]
12. Sangermano R, Bax NM, Bauwens M, van den Born LI, De Baere E, Garanto A, Collin RW, Goercham-Ramlal AS, den Engelsman-van Dijk AH, Rohrschneider K, Hoyng CB, Cremers FP, and Albert S, "Photoreceptor Progenitor mRNA Analysis Reveals Exon Skipping Resulting from the ABCA4 c.5461–10T->C Mutation in Stargardt Disease," *Ophthalmology* 123, 1375–1385 (2016). [PubMed: 26976702]
13. Singh G, and Cooper TA, "Minigene reporter for identification and analysis of cis elements and trans factors affecting pre-mRNA splicing," *Biotechniques* 41, 177–181 (2006). [PubMed: 16925019]
14. Gamundi MJ, Hernan I, Muntanyola M, Maseras M, Lopez-Romero P, Alvarez R, Dopazo A, Borrego S, and Carballo M, "Transcriptional expression of cis-acting and trans-acting splicing mutations cause autosomal dominant retinitis pigmentosa," *Human mutation* 29, 869–878 (2008). [PubMed: 18412284]
15. Nathans J, and Hogness DS, "Isolation and nucleodies sequence of the gene encoding human rhodopsin," *Proceedings of the National Academy of Sciences, USA* 81, 4851–4855 (1984).
16. Nathans J, Thomas D, and Hogness DS, "Molecular genetics of human color vision: the genes encoding blue, green, and red pigments," *Science* 232, 193–202 (1986). [PubMed: 2937147]
17. Kinnear PR, and Sahraie A, "New Farnsworth-Munsell 100 hue test normal of normal observers for each year of age 5–22 and for age decades 30–70," *British Journal of Ophthalmology* 86, 1408–1411 (2002). [PubMed: 12446376]
18. Lek M, Karczewski KJ, Minikel EV, Samocha KE, Banks E, Fennell T, O'Donnell-Luria AH, Ware JS, Hill AJ, Cummings BB, Tukiainen T, Birnbaum DP, Kosmicki JA, Duncan LE, Estrada K, Zhao F, Zou J, Pierce-Hoffman E, Berghout J, Cooper DN, Deflaux N, DePristo M, Do R, Flannick J, Fromer M, Gauthier L, Goldstein J, Gupta N, Howrigan D, Kiezun A, Kurki MI, Moonshine AL, Natarajan P, Orozco L, Peloso GM, Poplin R, Rivas MA, Ruano-Rubio V, Rose SA, Ruderfer DM, Shakir K, Stenson PD, Stevens C, Thomas BP, Tiao G, Tusie-Luna MT, Weisburd B, Won HH, Yu D, Altshuler DM, Ardissino D, Boehnke M, Danesh J, Donnelly S, Elosua R, Florez JC, Gabriel SB, Getz G, Glatt SJ, Hultman CM, Kathiresan S, Laakso M, McCarroll S, McCarthy MI, McGovern D, McPherson R, Neale BM, Palotie A, Purcell SM, Saleheen D, Scharf JM, Sklar P, Sullivan PF, Tuomilehto J, Tsuang MT, Watkins HC, Wilson JG,

- Daly MJ, and MacArthur DG, "Analysis of protein-coding genetic variation in 60,706 humans," *Nature* 536, 285–291 (2016). [PubMed: 27535533]
19. Pagani F, and Baralle FE, "Genomic variants in exons and introns: identifying the splicing spoilers," *Nat Rev Genet* 5, 389–396 (2004). [PubMed: 15168696]
  20. Ohno K, Takeda J-I, and Masuda A, "Rules and tools to predict the splicing effects of exonic and intronic mutations," *Wiley interdisciplinary reviews. RNA* 9, 10.1002/wrna.1451 (2018).
  21. Schwarze U, Hata R-I, McKusick VA, Shinkai H, Hoyme HE, Pyeritz RE, and Byers PH, "Rare autosomal recessive cardiac valvular form of Ehlers-Danlos syndrome results from mutations in the COL1A2 gene that activate the nonsense-mediated RNA decay pathway," *American journal of human genetics* 74, 917–930 (2004). [PubMed: 15077201]
  22. Pokorny J, Smith VC, and Verriest G, "Congenital color defects," in *Congenital and Acquired Color Vision Defects*, Pokorny J, Smith V, Verriest G, and Pinckers A, eds. (Grune & Stratton, 1979), pp. 183–241.
  23. Roman-Sanchez R, Wensel TG, and Wilson JH, "Nonsense mutations in the rhodopsin gene that give rise to mild phenotypes trigger mRNA degradation in human cells by nonsense-mediated decay," *Exp Eye Res* (2015).
  24. Ueyama H, Muraki-Oda S, Yamade S, Tanabe S, Yamashita T, Shichida Y, and Ogita H, "Unique haplotype in exon 3 of cone opsin mRNA affects splicing of its precursor, leading to congenital color vision defect," *Biochem Biophys Res Commun* 424, 152–157 (2012). [PubMed: 22732407]
  25. Gardner JC, Liew G, Quan YH, Ermetal B, Ueyama H, Davidson AE, Schwarz N, Kanuga N, Chana R, Maher ER, Webster AR, Holder GE, Robson AG, Cheetham ME, Liebelt J, Ruddle JB, Moore AT, Michaelides M, and Hardcastle AJ, "Three different cone opsin gene array mutational mechanisms with genotype-phenotype correlation and functional investigation of cone opsin variants," *Human mutation* 35, 1354–1362 (2014). [PubMed: 25168334]
  26. Greenwald S, Kuchenbecker JA, Rowlan JS, Neitz J, and Neitz M, "Role of a dual splicing and amino acid code in myopia, cone dysfunction and cone dystrophy associated with L/M opsin interchange mutations," *TVST* 6, 2 (2017).
  27. Hofer H, Carroll J, Neitz J, Neitz M, and Williams DR, "Organization of the human trichromatic cone mosaic," *Journal of Neuroscience* 25, 9669–9679 (2005). [PubMed: 16237171]
  28. Stockman A, "Colour Vision Research Laboratory and Database."
  29. Carroll J, McMahan C, Neitz M, and Neitz J, "Flicker-photometric electroretinogram estimates of L : M cone photoreceptor ratio in men with photopigment spectra derived from genetics," *Journal of the Optical Society of America A* 17, 499–509 (2000).
  30. Verriest G, Van Laethem J, and Uvijls A, "A new assessment of the normal ranges of the Farnsworth-Munsell 100-hue test scores," *Am J Ophthalmol* 93, 635–642 (1982). [PubMed: 6979252]
  31. Verriest G, "Further studies on acquired deficiency of color discrimination," *Journal of the Optical Society of America* 53, 185–195 (1963). [PubMed: 13996879]
  32. Smith VC, Pokorny J, and Pass AS, "Color-axis determination on the Farnsworth-Munsell 100-Hue Test," *American Journal of Ophthalmology* 100, 176–182 (1985). [PubMed: 3874549]
  33. Shinomori K, Panorgias A, and Werner JS, "Discrimination thresholds of normal and anomalous trichromats: Model of senescent changes in ocular media density on the Cambridge Colour Test," *Journal of the Optical Society of America. A, Optics, image science, and vision* 33, A65–76 (2016).
  34. Paramei GV, and Oakley B, "Variation of color discrimination across the life span," *Journal of the Optical Society of America. A, Optics, image science, and vision* 31, A375–384 (2014).

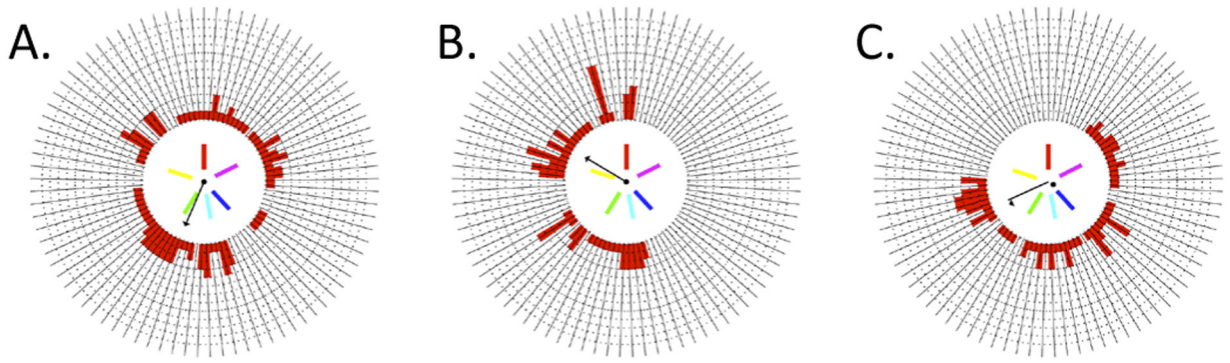


**Figure 1.**  
FM100 hue test results for the proband, subject 4028 (A), her sister, subject 4069 (B) and her mother (C), subject 5204.

Author Manuscript

Author Manuscript

Author Manuscript

Author Manuscript

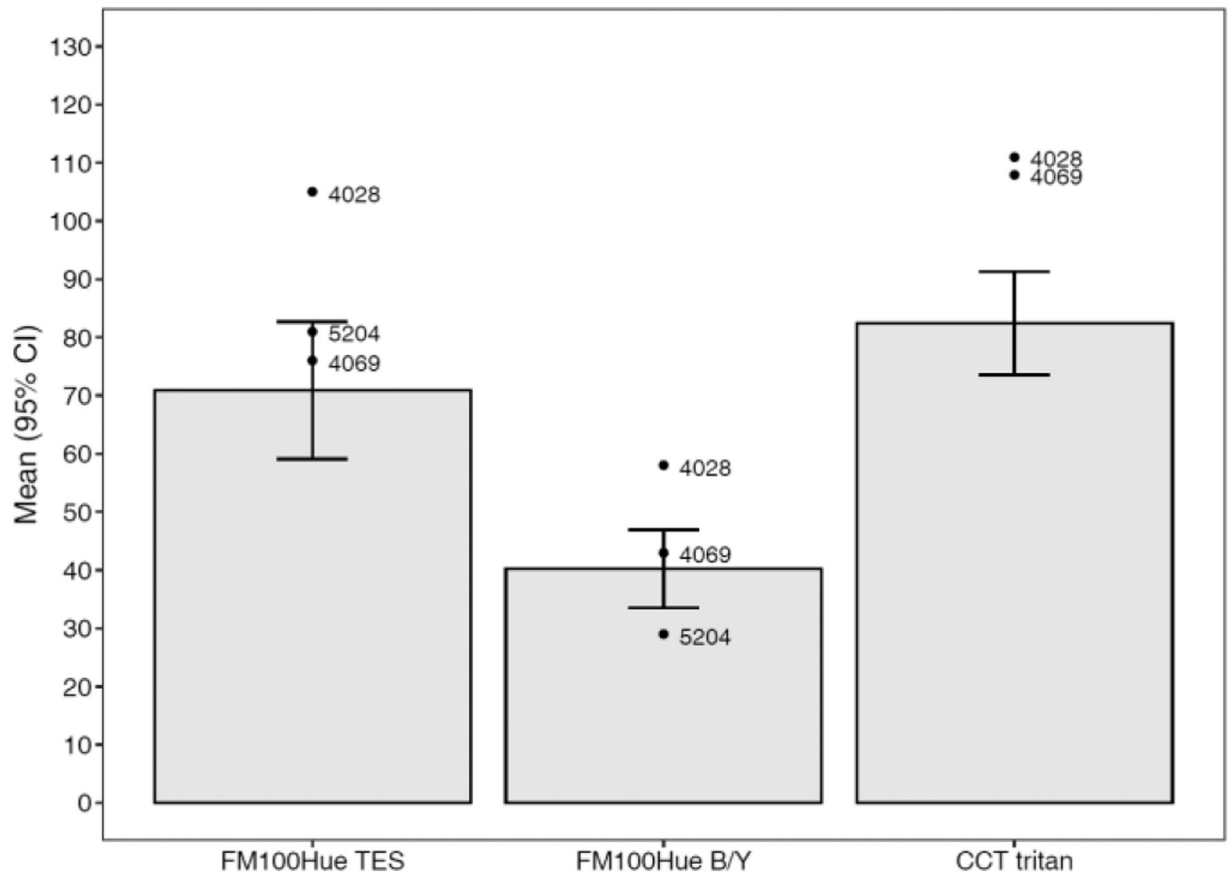


**Figure 2.**

Results from color vision testing for each of the potential tritan subjects plotted along with the mean and 95% confidence intervals (CI) for the normal trichromats for the FM100 Hue test (TES and B/Y partial error score,  $n=50$ ) and CCT tritan vector ( $n=49$ ). Subject 4028 made significant tritan errors compared with normal trichromats on both tests. Her sister (4069) made significant errors along the CCT tritan vector only. Her mother (5204) was within the 95% CI on the FM100 Hue, she was not tested on the CCT.

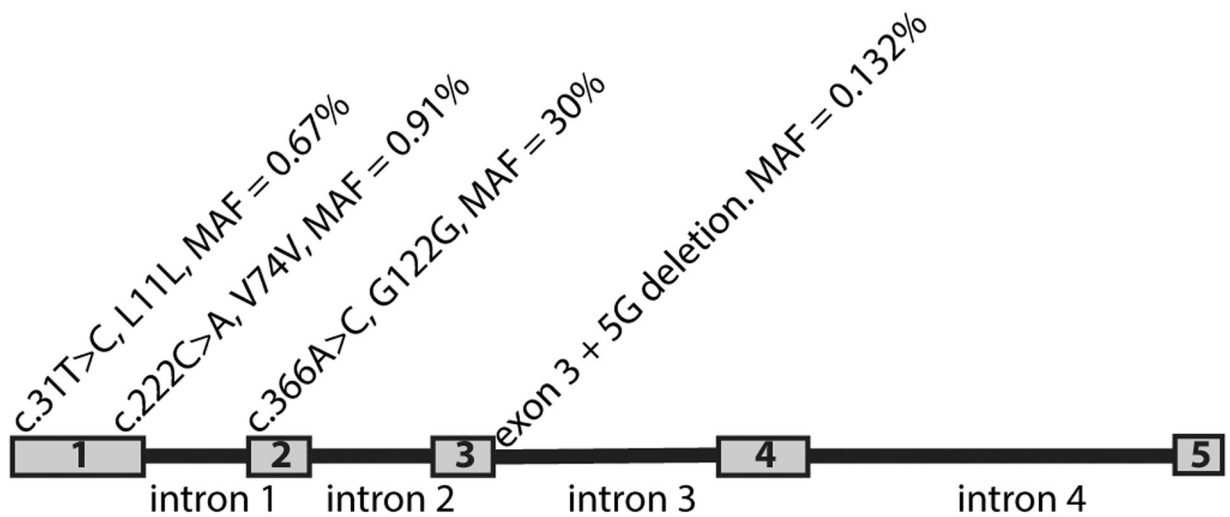


**Figure 3.**

Diagram of the *OPN1SW* gene. The gray boxes represent exons, black lines represent introns. Locations of each nucleotide variation identified in the subjects in this study are shown using conventional notation. For example, c.31C>T in exon 1 indicates a polymorphism at nucleotide position 31 (c.31), affecting the amino acid at position 11. The major allele at c.31 is C, the minor allele is T (c.31C>T). The the major and minor alleles specify the amino acid Leucine, indicated by L11L. The population frequency of the minor allele (MAF), c.31T, is 0.67%. The exon 3+5G deletion is a deletion of the 5<sup>th</sup> nucleotide of intron 3.

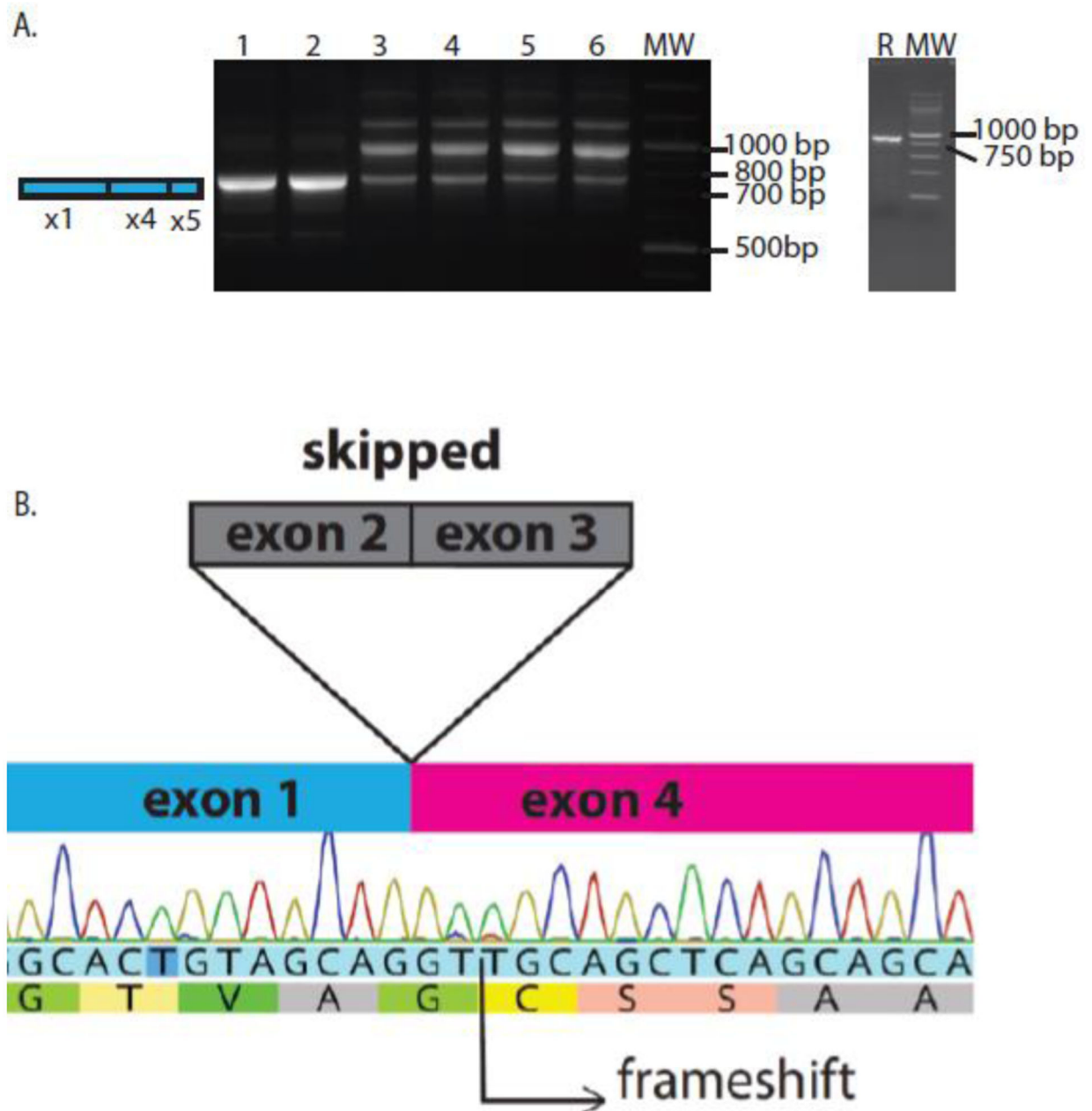


**Figure 4.**

A. Splicing isoforms of the normal and exon 3 +5G deletion mutant *OPN1SW* gene A. Plasmids carrying either the exon3+5G deletion *OPN1SW* allele, a normal *OPN1SW* allele, or a control rhodopsin gene were transfected into HEK293 cells. RNA was isolated, and converted to DNA, and the splicing isoforms analyzed on a 1.5% agarose gel. On the left gel, lanes 1 and 2 are duplicate splicing assays on exon 3 +5G deletion, lanes 3 and 4 are duplicate splicing assays on a normal *OPN1SW* gene from one normal subject, lanes 5 and 6 are duplicate splicing assays on a normal *OPN1SW* from another normal subject. On the right gel lane R is the splicing assay for the rhodopsin control. For both gels MW = molecular weight markers, and the sizes are labeled to the right. The exon 3 +5G deletion



gave a single splicing isoform in which exons 2 and 3 were skipped and the sequence is shown in B. Sequencing electropherogram of the exon 3 +5G deletion splicing product. Exon 1 is spliced to exon 4, which causes the protein code to go out of frame at the location of the arrow. Nucleotide identities for each peak are shown, and underneath is the single letter amino acid code. G = glycine, T = threonine, V = valine, A = alanine, C = cysteine, S = serine.

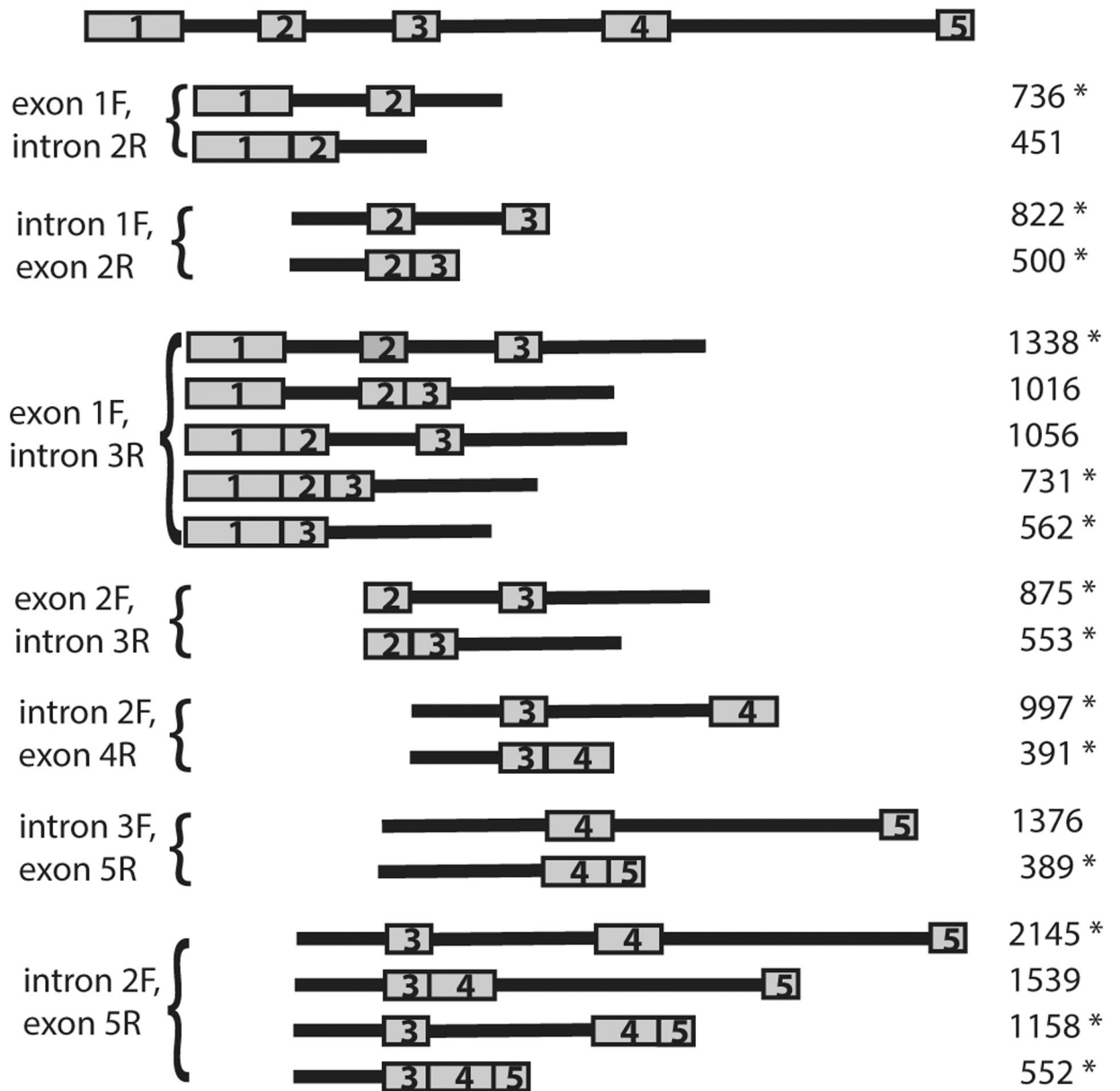


**Figure 5.** Potential splicing intermediates for each of the primer pairs indicated in column 1. The primer sequences are given in Table 2. Gray boxes indicate exons, black lines indicate introns. The top is a diagram to scale of the *OPN1SW* gene, below which are shown possible splicing intermediates. The right column shows the sizes in base pairs of the PCR products expected for each of the potential splicing intermediates. The asterisk indicates a true splicing intermediate (observed in Figure 6), and those without an asterisk were not true intermediates (not observed in Figure 6). See Figure 3 for intron numbering convention.

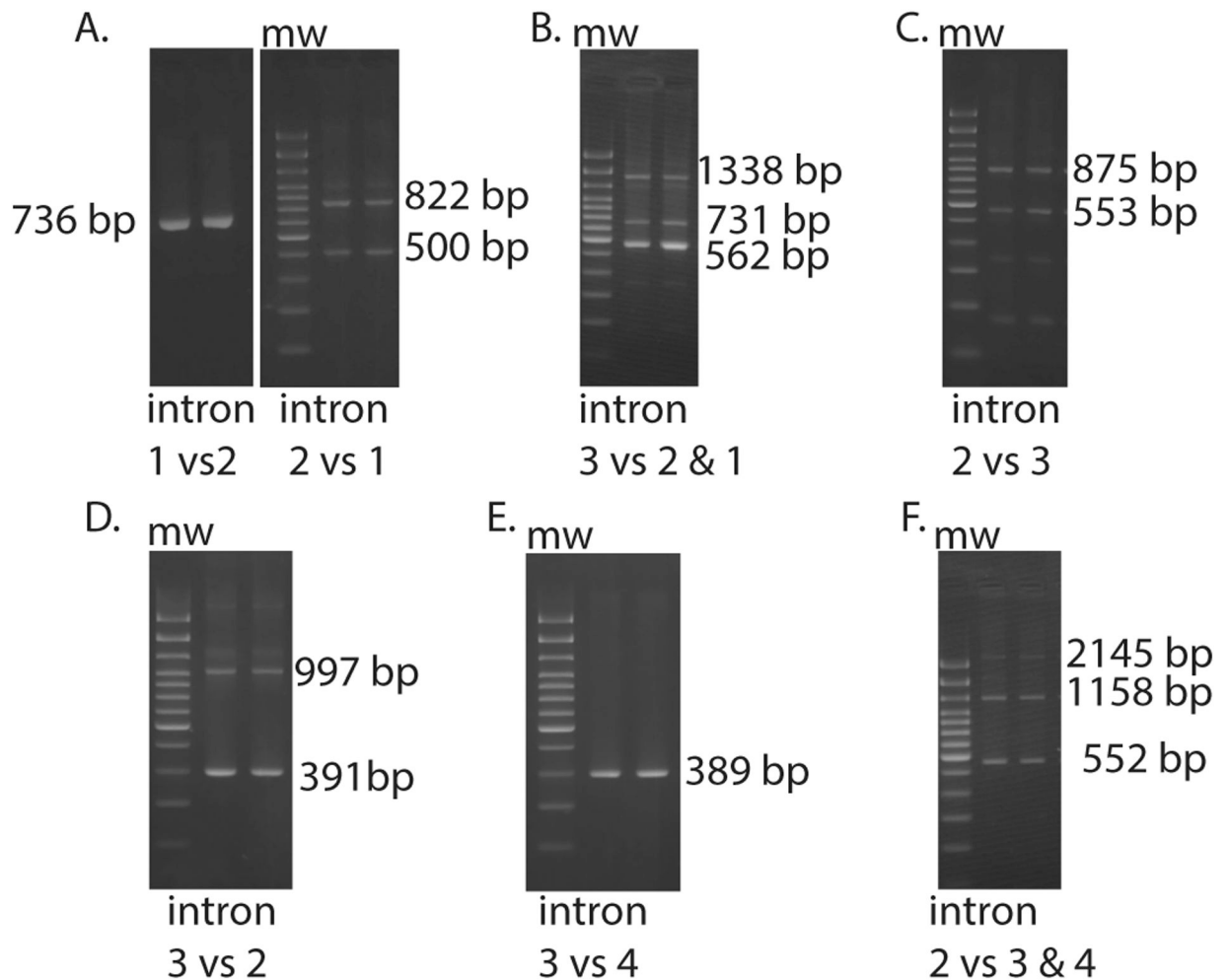


**Figure 6.**

Splicing isoforms observed with primers pairs given in Table 2 and Figure 5. See Figure 5 for all possible splicing isoforms. For each primer pair, the splicing assay was performed in triplicate, only duplicates are shown to conserve space. For each set of primers use, the reactions were done in the absence of reverse transcriptase (not shown) to verify the absence of contaminating DNA. Forward (F) and Reverse (R) primers pairs used in each panel were: A. Left panel: exon 1F, intron 2R, Right panel: intron 1F, exon 3R. B. exon1F, intron 3R, C. exon 2F, intron 3R, D. intron 2F, exon 4R, E. intron 3F, exon 5R, F. intron 2F, exon 5R. For each panel, the size and structure of splicing isoform observed are indicated. MW is molecular weight marker (Invitrogen 100 bp ladder, from top to bottom in bp: 2000, 1500, 1200, 1000, 900, 800, 700, 600, 500, 400, 300, 100).

**Table 1:**Primers for amplifying *OPN1SW* exons

Amplicon	Primers
Exon 1	Forward: AAGAGGACTCAGAGGAGGGTGTG Reverse: CTAACCCCTTTTCCCCTGC
Exon 2	Forward: GCCCATTAT <u>I</u> CTCACATTTCACC* Reverse: CACCACTGCCCTGCACTCT
Exon 3	Forward: GGAGAACAATCCAGGCATCT Reverse: TCTTCCCTGACTATCAAATGCCA
Exon 4	Forward: AGATGTGATGCTTCCGTGCT Reverse: GACCATAGGAATGTGAATAAAGAGC
Exon 5	Forward: TCTGCCAAGGTTATCTCCAATTG Reverse: AAAATTTAATTCTAGCTGTTGCAAAC

\* There is one mismatch (underlined) between the primer and the *OPN1SW* reference sequence.

**Table 2:**PCR primers to investigate the order of intron removal from *OPN1SW*

Introns	Primer sequences, direction*, location and melting temperature
1 vs 2	F 5'CCTCAACTACATTCTGGTCAACGTGTCCTTCG Location: exon 1 Tm = 68.4
	R 5'CACTGCCCTTTCGCCTCATATTGCAACTCTTA Location: intron 2 Tm = 68.6
2 vs 1	F 5'GGGGAAATGAGTCTGGTGCTTTTAAAATACTGG Location: intron 1 Tm = 67.5
	R 5'AGGGAGAGAGGCACAATGAAGCAGAAGATG Location: exon 3 Tm = 67.9
2 vs 3	F 5'CTGGCCTTTGAGCGCTACATTGTCATCTG Location: exon 2 Tm = 67.8
	R 5'GCCCGGTCTCTGGATGCTTTTCTGTG Location: intron 3 Tm = 67.7
3 vs 2	F 5'GAGTCCAGTGAGCAAGTGTTT Location: intron 2 Tm = 58.4
	R 5'GGAGAAGAATGAAGGAATGGTGAC Location: exon 4 Tm = 59.4
4 vs 3	F 5'GAAAAAGAGAGATGTGATGCTTCCGTG Location: intron 3 Tm = 63.0
	R 5'AACTGGGTAGACGAGACAGTAGAAAC Location: exon 5 Tm = 62.3
3 vs 2 vs 1	F 5'CCTCAACTACATTCTGGTCAACGTGTCCTTCG Location: exon 1 Tm = 68.4
	R 5'GCCCGGTCTCTGGATGCTTTTCTGTG Location: intron 3 Tm = 67.7
2 vs 3 vs 4	F 5'GAGTCCAGTGAGCAAGTGTTT Location: intron 2 Tm = 58.4
	R 5'AACTGGGTAGACGAGACAGTAGAAAC Location: exon 5 Tm = 62.3

\* F is forward, R is reverse

**Table 3.**

## Color vision test results

<b>Subject ID</b>	<b>4028</b>	<b>4069</b>	<b>5204</b>
FM100 TES	105	76	81
FM100 B/Y TPES	58	43	29
CCT Protan	66	59	ND
CCT Deutan	63	79	ND
CCT Tritan	111	118	ND
Rayleigh MP	39.2	40.45	ND
Rayleigh MR	0.8	0.9	ND

Author Manuscript

Author Manuscript

Author Manuscript

Author Manuscript

**Table 4.**Combinations of polymorphisms in *OPN1SW* genes

No. of Subjects	c.31	c.222	c.366	Other mutations
20 (3M, 17F)	C	C	AA	None
9 (3M, 6F)	C	C	CC	None
18 (5M, 13F)	C	C	AC	None
1 (F)	T	C	AC	None
1 (F)	C	A	AA	None
3 (F)	C	C	AA	Exon 3 +5G deletion

Author Manuscript

Author Manuscript

Author Manuscript

Author Manuscript